(b) From 2. A solution of 223 mg (0.216 mmol) of **2** in 10 mL of toluene was saturated with CO. The red microcrystalline **3**, which precipitated after 8 h, was filtered and vacuum-dried.

(c) From $Pd(PCy_3)_2$. The absorption of CO by a solution containing 434 mg (0.652 mmol) of $Pd(PCy_3)_2$ in 20 mL of toluene was measured with a gas-volumetric apparatus; 0.645 mmol of CO was absorbed. From the solution a red microcrystalline solid precipitated, which was shown to be identical with a sample prepared by method a.

X-ray Crystallography. Crystal data and details of measurements for **1** and **2** are reported in Table I.

Diffraction intensities were collected at room temperature by the $\omega/2\theta$ scan method of an Enraf-Nonius CAD-4 diffractometer with Mo Kα radiation (λ = 0.71069 Å) and reduced to F_o values.

The structures were solved by Patterson and direct methods and refined by full-matrix least-squares calculations. For all computations the SHELX76 and SHELX86[13,14] packages of crystallographic programs were used with the analytical scattering factors, corrected for real and imaginary parts of anomalous dispersions, taken from ref 14b. Thermal vibrations were treated anisotropically.

In both compounds the H atoms bound to Pd(II) were found in a final difference map by using a reduced reflection sphere ($(\sin\theta)/\lambda$ = 0.3) and kept at their observed distances [1.57 (2) and 1.46 (2) Å, respectively] from Pd.

Also, the phenol and pentafluorophenol O-bound H atoms were directly located and kept at their found positions of 1.18 and 0.89 Å, respectively, from O43. All the remaining H atoms were added in calculated positions (C–H = 1.08 Å) and refined riding on the corresponding C atoms. Common temperature factors were refined for chemically equivalent H atoms, while the H(hydride) and H(bridging) atoms were treated independently.

Final difference Fourier maps showed residual peaks lower than 1 e $Å^{-3}$ in both compounds. Final atomic coordinates for **1** and **2** are listed in Tables II and III, while relevant bond distances and angles are reported in Table IV.

Absorption correction was made by applying the Walker and Stuart[15] method after a complete structural model was obtained and all atoms were refined isotropically for **1**. For **2** an empirical absorption correction was applied by measuring scans at intervals of 10° around the diffraction vectors of eight selected reflections near χ = 90° (transmission range 71–100%).

Registry No. **1**, 112469-70-2; **2**, 119455-96-8; **3** (n = 3), 95246-51-8; $Pd(PCy_3)_2$, 33309-88-5; PhOH, 108-95-2; C_6F_5OH, 771-61-9; CH_3OH, 67-56-1; *i*-PrOH, 67-63-0.

Supplementary Material Available: Hydrogen atom coordinates (Tables S-I and S-II), anisotropic thermal parameters (Tables S-III and S-IV), bond distances and angles (Tables S-V and S-VI), and crystal data and intensity collection parameters (Table S-IX) (74 pages); observed and calculated structural factors (Tables S-VII and S-VIII) (78 pages). Ordering information is given on any current masthead page.

(13) Sheldrick, G. M. "SHELX86"; University of Gottingen: Gottingen, FRG, 1986.
(14) (a) Sheldrick, G. M. "SHELX76"; University of Cambridge, Cambridge, England, 1976. (b) *International Tables for X-ray Crystallography*; Kynoch: Birmingham, England, 1974; Vol. IV, pp 99, 149.
(15) Walker, N.; Stuart, D. *Acta Crystallogr., Sect. A* **1983**, 158.

Contribution from the Institut de Chimie Minérale et Analytique, Université de Lausanne, 3, Place du Château, CH-1005 Lausanne, Switzerland, Department of Chemistry, University of Stirling, Stirling FK9 4LA, Scotland, U.K., and Institut de Cristallographie, Université de Lausanne, CH-1015 Lausanne, Switzerland

Crystal Structure of and Mechanism of Water Exchange on $[Mo_3O_4(OH_2)_9]^{4+}$ from X-ray and Oxygen-17 NMR Studies

David T. Richens,*[1a] Lothar Helm,[1b] Pierre-André Pittet,[1b] André E. Merbach,*[1b] Francesco Nicolò,[1c] and Gervais Chapuis*[1c]

Received June 14, 1988

Acid dissociation and water exchange on $[Mo_3O_4(OH_2)_9]^{4+}$ have been studied by ^{17}O NMR and UV–visible spectrophotometry in noncomplexing acidic aqueous solution. Contrary to an earlier report, the oxygen atoms of the "core" are extremely inert with no exchange observed on either over a 2-year period. Exchange at the d-H_2O ligands, trans to the μ_2-bridging oxygen atoms of the "core", occurs readily (k_{OH}^{298} = 1.6 × 10^2 s^{-1}) and much faster than that occurring at the c-H_2O, trans to the capping oxygen (k_{OH}^{298} = 1.5 × 10^{-3} s^{-1}). A mechanism of exchange for both waters involving solely the same conjugate base $[Mo_3O_4(OH_2)_8(OH)]^{3+}$ is relevant. The positive $\Delta S^{\ddagger}$ value (+35 J K^{-1} mol^{-1}) for the d-H_2O exchange and comparison with available data for 1:1 anation reactions of $[Mo_3O_4(OH_2)_9]^{4+}$ with NCS^- and $HC_2O_4^-$ add support for an I_d mechanism. Chemical shifts for both the c- and d-H_2O ^{17}O NMR resonances followed as a function of H^+ concentration confirmed that the relevant deprotonation occurred uniquely at a d-H_2O. Values for $K_a^{298}(Mo_3O_4^{4+})$, determined from the kinetic treatment (0.31 M) and from UV–visible spectrophotometry (0.24 M), were in satisfactory agreement and indicative of high acidity at the d positions. The compound $[Mo_3O_4(OH_2)_9](CH_3C_6H_4SO_3)_4 \cdot 13H_2O$ crystallizes in the monoclinic space group *Cc*: a = 31.99 (1) Å, b = 9.886 (2) Å, c = 17.789 (5) Å, β = 99.67 (2)°. The final agreement was R = 0.059 with 5183 observed reflections. The packing is mainly characterized by the large number of crystallization water molecules and H-bond interactions. It consists of alternate layers of opposite charge.

Introduction

The aqua ion of molybdenum(IV), first isolated by Souchay in 1966,[2] is now well established as containing the cyclic trinuclear metal cluster unit $[Mo_3O_4(OH_2)_9]^{4+}$ (**1**). Thus, X-ray crystal-

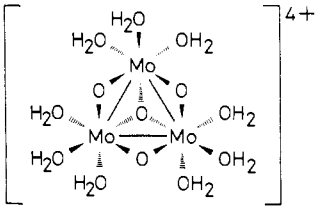

1

lographic characterization of Mo(IV) complexes such as $[Mo_3O_4(C_2O_4)_3(OH_2)_3]^{2-}$[3,4] and $[Mo_3O_4(NCS)_8(OH_2)]^{4-}$[5] together with isotopic labeling of the core μ_2- and μ_3-oxygen atoms with ^{18}O[4] and, more recently, ^{17}O[6] have demonstrated that the trinuclear unit is retained for solutions of the red aqua ion.

The two types of "core" oxygen atom labeled "a" and "b" and coordinated H_2O ligands "c" and "d" can be readily distinguished in the 4 atom % enriched ^{17}O NMR spectrum of the Mo(IV) ion

(1) (a) University of Stirling. Present address of D.T.R.: Department of Chemistry, University of St. Andrews, St. Andrews KY16 9AG, Scotland, U.K. (b) Institut de Chimie Minérale et Analytique, Université de Lausanne. Taken in part from the Ph.D. thesis of P.-A.P. (c) Institut de Cristallographie, Université de Lausanne.
(2) Souchay, P.; Cadiot, M.; Duhameaux, M. *C. R. Seances Acad. Sci., Ser. C* **1966**, *262*, 1524.
(3) Bino, A.; Cotton, F. A.; Dori, Z. *J. Am. Chem. Soc.* **1978**, *100*, 5252.
(4) Rodgers, K. R.; Murmann, R. K.; Schlemper, E. O.; Shelton, M. E. *Inorg. Chem.* **1985**, *24*, 1313.

0020-1669/89/1328-1394$01.50/0

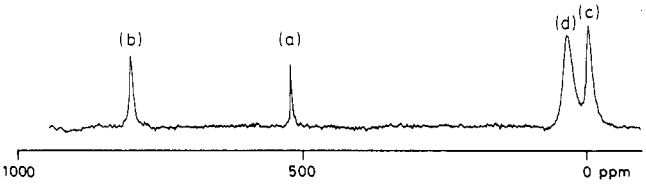

Figure 1. 54.2-MHz ^{17}O NMR spectrum (298.2 K) of $[Mo_3O_4(OH_2)_9]^{4+}$ (0.013 M), in Hpts (0.44 M) containing $Mn(pts)_2$ (0.11 M). The peaks are attributed to μ_2- (b) and μ_3-^{17}O (a) (3.3 atom %) and $H_2{}^{17}O$ (4 atom %) trans to the μ_3-oxo (c) and trans to the μ_2-oxo groups (d); spline functions were used to subtract base-line rolling.

(Figure 1) and assigned on the basis of chemical shift and peak integrations of the individual resonances.[6]

Since its first isolation the ion has been the subject of a number of studies with regard to the mechanisms of both redox[7-9] and complexation reactions[4,10,11] Sykes and colleagues have reported kinetic studies involving complexation reactions with NCS^-[10,11] and it seems that statistical factors, involved with substitution at three equivalent Mo atoms, are relevant.[11]

Further recent work by the Sykes group with regard to complexation with both oxalate and NCS^- (conducted while this work was in progress) favors a common pathway for substitution involving only the conjugate base ion $[Mo_3O_4(OH_2)_8(OH)]^{3+}$.[12] Such behavior allowed a kinetic determination of the relevant acid dissociation constant $K_a{}^{298}(Mo_3O_4{}^{4+})$ of 0.42 M,[12] indicating much higher acidity in the coordinated water ligands than had been previously supposed for such an already extensively hydrolyzed species.

In extending the unique power of ^{17}O NMR in selectively probing the solution chemistry of different oxygen atoms in an oligomeric oxo aqua ion, we wish to report here the results of a study of water exchange with the oxygen atoms of $[Mo_3O_4(OH_2)_9]^{4+}$. The acid dissociation of $[Mo_3O_4(OH_2)_9]^{4+}$ has also been further addressed and further values for $K_a{}^{298}(Mo_3O_4{}^{4+})$ have been independently determined from both the water-exchange kinetics and UV–visible spectrophotometry. The precise location of the relevant site of deprotonation has been determined. The results support the recent findings of the Sykes group with regard to high acidity in the coordinated water ligands and the suggestion that an I_d mechanism is relevant for substitution reactions on this ion.[12] An X-ray crystal structure study was undertaken to provide a possible explanation of the solution properties of $[Mo_3O_4(OH_2)_9]^{4+}$.

Experimental Section

Preparation of Solutions. Stock solutions of $[Mo_3O_4(OH_2)_9]^{4+}$ were prepared by a slight modification of the previously reported method[13] in order to obtain the higher concentrations of Mo(IV) (>0.1 M/$Mo_3O_4{}^{4+}$) needed for the NMR experiments. Sodium molybdate (2.42 g, 0.01 mol, Fluka puriss) and potassium hexachloromolybdate(III) (9.5 g, 0.022 mol) were heated together to 353 K for 1–2 h in deoxygenated HCl solution (2.0 M, 50 cm^3). The resulting mixture was then diluted to $[H^+] = 0.5$ M with water and *p*-toluenesulfonic acid (tosylic acid, Hpts, Fluka puriss) to a final volume of 500 cm^3, left for 24 h to allow complete aquation of coordinated Cl^-, and then loaded onto a column (20 cm × 1 cm) of Dowex 500W-X2 cation exchange resin (H^+ form). Any residual Mo(V) or $Mo_3O_4Cl_n{}^{(4-n)+}$ species were then removed by successive washing of the column with 0.5 and 1.0 M Hpts solutions until the washings were colorless and free of Cl^- ($AgNO_3$). Concentrated solutions of $[Mo_3O_4(OH_2)_9]^{4+}$ were then collected by slow displacement elution with a solution of 0.25 M $La(pts)_3$ in 1.0 M Hpts. The presence of La^{3+} in each fraction was monitored by dropwise addition to solutions of oxalic acid. Concentrations of $Mo_3O_4{}^{4+}$ as high as 0.2 M can be collected in the main intense red fraction (5–10 cm^3). For conditions of higher acidity, elution was also carried out with saturated (5.0 M) solutions of Hpts, giving concentrations up to 0.13 M. Solutions of $Mo_3O_4{}^{4+}$ at $[H^+] = 2.0$ M were standardized as in previous studies at the peak maximum of 505 nm ($\epsilon = 189\ M^{-1}\ cm^{-1}$).[13]

Samples of Li(pts), $La(pts)_3$, and $Mn(pts)_2$ were prepared by dissolution of Li_2CO_3, La_2O_3, and $MnCO_3$ (Fluka puriss), respectively, in Hpts solutions followed by recrystallization twice from water. Trifluoromethanesulfonic acid (Htfms) (Fluka) was distilled under reduced pressure (bp 353 K (10 mmHg)). Solutions of Li(tfms) were similarly prepared as for Li(pts). Salt solutions were standardized by ion exchange with a column of Dowex 50W-X8 resin (H^+ form) and titration of the liberated H^+. Background H^+ concentrations in solutions of $Mo_3O_4{}^{4+}$ and La^{3+} were similarly determined by difference. Normal water was doubly distilled. Samples of oxygen-17 enriched water (10–20 atom %) were obtained from Yeda, Israel.

UV–visible spectra were recorded on Perkin-Elmer Lambda 5 and 7 instruments in both 0.1- and 1.0-cm quartz cells.

Determination of the Acid Dissociation Constant, K_a, for $[Mo_3O_4(OH_2)_9]^{4+}$. The concentration of H^+ in solutions of $[Mo_3O_4(OH_2)_9]^{4+}$ was adjusted by rapid dilution of a 0.06 M $Mo_3O_4{}^{4+}$ and 1.4 M Hpts solution into solutions of Li(pts) to maintain an ionic strength of 2.0 M. This method had the virtue of decreasing the $[Mo_3O_4{}^{4+}]$ concurrent with the decreasing concentration of H^+, thus minimizing the formation of oligomeric products. Moreover, if the H^+ concentration is kept at a constant 20-fold excess over $Mo_3O_4{}^{4+}$ during the dilution, the increase (maximum 5%) in $[H^+]$ as a result of acid dissociation of $[Mo_3O_4(OH_2)_9]^{4+}$ can be neglected. An UV–visible spectrum of the resulting solution was recorded within 2 min over the range 320–680 nm at 298.2 ± 0.1 K. The extinction coefficient at the peak maximum of 505 nm was then evaluated as a function of $[H^+]$. Spectra for $Mo_3O_4{}^{4+}$ solutions at $[H^+] > 1.4$ M were also recorded but without ionic strength control. The data were successfully fitted as a function of $[H^+]$ to eq 1 by an iterative treatment with K_a, $\epsilon^{505}(Mo_3O_4{}^{4+})$, and $\epsilon^{505}(Mo_3O_4OH^{3+})$ as adjustable parameters.

$$\epsilon^{505}{}_{obs} = \frac{\epsilon^{505}(Mo_3O_4{}^{4+})\ [H^+] + \epsilon^{505}(Mo_3O_4OH^{3+})\ K_a}{[H^+] + K_a} \quad (1)$$

^{17}O NMR Measurements. All ^{17}O NMR spectra were recorded on a Bruker AM-400 spectrometer working at 54.24 MHz and using 10-mm o.d. sample tubes. Thermostating of the samples was achieved by blowing a stream of air or N_2 through the probe. The temperature (±0.5 K) was measured by a substitution technique.[14] According to the different experiments performed, total spectra widths of 40–83 kHz with 1K–4K data points for the FIDs (10^4–10^5 transients added) were used. The pulse width varied between 7 and 14 μs. Mn^{2+} (0.1 M) was added to all samples to flatten out the large bulk water resonance line.[15] All ^{17}O chemical shifts were measured with respect to $CF_3SO_3^-$ (+159 ppm) and reported relative to bulk water.

To monitor the exchange of μ_3- and μ_2-oxygens of the "core", spectra of ^{17}O core-enriched $Mo_3O_4{}^{4+}$ samples[6] in natural-abundance water and of natural-abundance $Mo_3O_4{}^{4+}$ samples in ca. 5% enriched $H_2{}^{17}O$ were recorded as a function of time (the sealed sample tubes being stored in the thermostated NMR room, at ca 295 ± 2 K).

In order to follow the exchange of the c-H_2O ligands, slow with respect to the NMR time scale, an isotopic labeling technique[16] was used. Two volumes (1 cm^3 each, at 298.0 ± 0.5 K) of acidified natural-abundance solutions of $[Mo_3O_4(OH_2)_9]^{4+}$ [μ = 1.0 M (Li(pts)] and of 10% $H_2{}^{17}O$ [μ = 1.0 M (Li(pts)), Mn^{2+} added] were rapidly mixed by use of a fast injection apparatus.[17] The $Mo_3O_4{}^{4+}$ concentration varied from 0.01 to 0.04 M and the $[H^+]$ from 0.062 to 0.645 M (not corrected for $Mo_3O_4{}^{4+}$ acid dissociation, maximum of ~12% at low $[H^+]$). Up to 80 spectra at 173-s time intervals were taken immediately after mixing (12 000 transients, 1K data points, 14-μs pulse width) to monitor the increase with time of the ^{17}O resonance line of the c-H_2O ligands.

The much faster exchange of the d-H_2O ligands was measured at different temperatures and different H^+ concentrations by observing the line broadening of the corresponding ^{17}O resonance. The $[H^+]$ was varied

(5) Schlemper, E. O.; Hussain, M. S.; Murmann, R. K. *Cryst. Struct. Commun.* **1982**, *11*, 89.
(6) Richens, D. T.; Helm, L.; Pittet, P.-A.; Merbach, A. E. *Inorg. Chim. Acta* **1987**, *132*, 85.
(7) Harmer, M. A.; Richens, D. T.; Soares, A. B.; Thornton, A. T.; Sykes, A. G. *Inorg. Chem.* **1981**, *20*, 4155.
(8) Paffett, M. T.; Anson, F. C. *Inorg. Chem.* **1983**, *22*, 1347.
(9) Richens, D. T.; Sykes, A. G. *Inorg. Chem.* **1982**, *21*, 418.
(10) Ojo, J. F.; Sasaki, Y.; Taylor, R. S.; Sykes, A. G. *Inorg. Chem.* **1976**, *15*, 1006.
(11) Kathirgamanathan, P.; Soares, A. B.; Richens, D. T.; Sykes, A. G. *Inorg. Chem.* **1985**, *24*, 2950.
(12) Ooi, B. L.; Sykes, A. G. *Inorg. Chem.* **1988**, *27*, 310.
(13) Richens, D. T.; Sykes, A. G. *Inorg. Synth.* **1985**, *23*, 130.
(14) Ammann, C.; Meier, P.; Merbach, A. E. *J. Magn. Reson.* **1982**, *46*, 319.
(15) Hugi-Cleary, D.; Helm, L.; Merbach, A. E. *J. Am. Chem. Soc.* **1987**, *109*, 4444.
(16) Helm, L.; Elding, L. I.; Merbach, A. E. *Helv. Chim. Acta* **1984**, *67*, 1453.
(17) Bernhard, P.; Helm, L.; Ludi, A.; Merbach, A. E. *J. Am. Chem. Soc.* **1985**, *107*, 312.

Table I. Atomic Coordinates ($\times 10^4$) and Equivalent Isotropic Displacement Parameters ($Å^2 \times 10^3$)

	x	*y*	*z*	*U*(eq)[a]
Mo(1)	0	2453 (1)	0	19 (1)
Mo(2)	85 (1)	376 (1)	802 (1)	19 (1)
Mo(3)	685 (1)	1979 (1)	828 (1)	20 (1)
O(1)	121 (3)	2318 (9)	1143 (6)	13 (3)
O(2)	−122 (3)	595 (10)	−250 (5)	21 (4)
O(3)	667 (3)	79 (10)	712 (6)	19 (3)
O(4)	551 (3)	2440 (9)	−227 (5)	15 (2)
O(5)	−57 (3)	4495 (9)	149 (5)	22 (3)
O(6)	−187 (3)	2942 (11)	−1193 (5)	28 (4)
O(7)	−674 (3)	2536 (10)	2 (6)	24 (4)
O(8)	−538 (3)	292 (10)	1061 (6)	25 (4)
O(9)	−8 (4)	−1755 (10)	589 (6)	30 (4)
O(10)	235 (3)	−211 (11)	1986 (5)	28 (4)
O(11)	974 (4)	1767 (10)	1994 (6)	30 (4)
O(12)	1326 (3)	1813 (10)	643 (6)	27 (4)
O(13)	848 (3)	4044 (10)	1058 (6)	25 (4)
S(1)	1517 (1)	4606 (4)	−518 (2)	27 (1)
O(14)	1267 (3)	5162 (10)	30 (6)	35 (4)
O(15)	1495 (3)	3119 (10)	−582 (6)	33 (4)
O(16)	1405 (4)	5258 (12)	−1260 (6)	41 (4)
C(17)	3374 (7)	5358 (24)	778 (12)	72 (9)
C(11)	2050 (5)	4925 (15)	−153 (8)	29 (5)
C(12)	2348 (6)	4349 (21)	−530 (12)	60 (8)
C(13)	2777 (6)	4502 (21)	−206 (12)	59 (8)
C(14)	2906 (6)	5211 (20)	450 (11)	46 (7)
C(15)	2591 (5)	5775 (22)	798 (10)	53 (8)
C(16)	2170 (6)	5658 (19)	509 (10)	47 (7)
S(2)	1657 (1)	−1216 (4)	1772 (2)	31 (1)
O(17)	1496 (4)	−2584 (12)	1712 (8)	58 (5)
O(18)	1450 (3)	−404 (12)	2296 (6)	35 (4)
O(19)	1633 (4)	−586 (12)	1026 (6)	47 (5)
C(27)	3510 (5)	−1272 (20)	3132 (9)	45 (7)
C(21)	2194 (5)	−1295 (15)	2176 (8)	29 (6)
C(22)	2315 (6)	−1457 (19)	2957 (9)	41 (6)
C(23)	2742 (7)	−1449 (19)	3254 (10)	51 (8)
C(24)	3060 (6)	−1283 (16)	2801 (10)	38 (6)
C(25)	2919 (6)	−1153 (20)	2035 (10)	46 (7)
C(26)	2499 (6)	−1154 (20)	1719 (10)	50 (8)
S(3)	−1148 (1)	785 (4)	−1712 (2)	29 (1)
O(20)	−918 (3)	1990 (11)	−1897 (6)	37 (4)
O(21)	−1109 (3)	629 (10)	−880 (5)	31 (4)
O(22)	−1020 (4)	−444 (12)	−2062 (6)	45 (5)
C(37)	−3018 (7)	1719 (25)	−2856 (13)	81 (11)
C(31)	−1688 (6)	1066 (16)	−2076 (9)	33 (6)
C(32)	−1956 (7)	21 (21)	−2091 (12)	64 (9)
C(33)	−2376 (7)	229 (23)	−2339 (11)	64 (9)
C(34)	−2539 (7)	1476 (23)	−2561 (12)	57 (8)
C(35)	−2254 (7)	2486 (22)	−2574 (13)	71 (9)
C(36)	−1823 (7)	2311 (19)	−2316 (13)	67 (9)
S(4)	−1333 (1)	4725 (4)	−4528 (2)	29 (1)
O(23)	−1214 (3)	5420 (12)	−3798 (6)	42 (4)
O(24)	−1090 (4)	5204 (11)	−5092 (6)	37 (4)
O(25)	−1308 (4)	3262 (10)	−4451 (6)	38 (4)
C(47)	−3168 (6)	6054 (23)	−5787 (11)	69 (9)
C(41)	−1867 (4)	5094 (16)	−4887 (8)	27 (5)
C(42)	−2178 (5)	4226 (16)	−4759 (9)	30 (6)
C(43)	−2593 (6)	4531 (19)	−5066 (9)	41 (6)
C(44)	−2702 (6)	5712 (22)	−5467 (9)	46 (7)
C(45)	−2392 (6)	6580 (19)	−5571 (10)	46 (7)
C(46)	−1964 (7)	6285 (17)	−5298 (10)	49 (8)
O(80)	−716 (4)	2094 (11)	−3382 (6)	33 (4)
O(81)	−92 (4)	4381 (11)	−3531 (6)	36 (4)
O(82)	−806 (3)	7706 (10)	−3170 (5)	29 (4)
O(83)	−769 (4)	8064 (11)	−304 (6)	36 (4)
O(84)	656 (3)	−662 (12)	−946 (6)	38 (4)
O(85)	769 (4)	−2841 (11)	−1791 (6)	35 (4)
O(86)	−121 (3)	9180 (11)	−1927 (6)	33 (4)
O(87)	1030 (4)	1461 (11)	−1598 (6)	41 (4)
O(88)	763 (4)	2694 (13)	−4657 (8)	54 (5)
O(89)	314 (4)	2597 (11)	−2287 (6)	38 (4)
O(90)	1002 (4)	4422 (11)	−2708 (6)	39 (4)
O(91)	−81 (4)	6173 (11)	−2353 (6)	43 (5)
O(92)	−276 (5)	6175 (14)	−908 (7)	75 (7)

[a] Equivalent isotropic *U* defined as one-third of the trace of the orthogonalized U_{ij} tensor.

between 0.350 and 0.776 M at a constant $[Mo_3O_4^{4+}]$ of 0.02 M. Samples at $[H^+] < 0.350$ M gave poor results consistent with formation of oligomeric products as the temperature was raised above 313 K. The temperature of the measurements varied from 283.5 to 339.0 K. A total of between 5×10^4 and 3×10^5 transients (4K data points, 14-μs pulse width) were added to get acceptable signal to noise ratios.

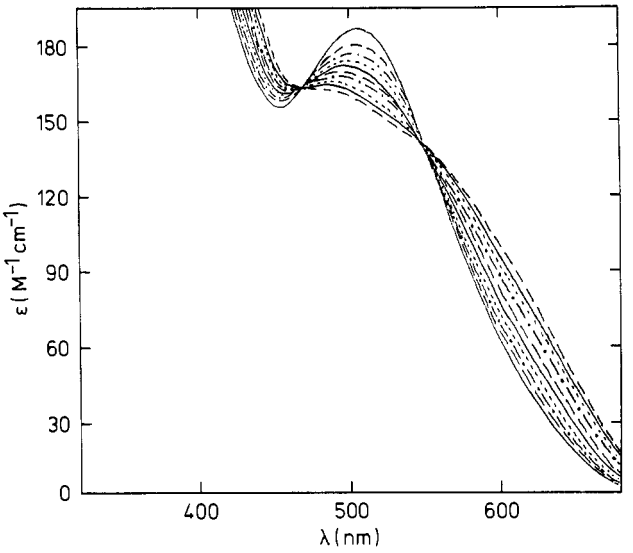

Figure 2. UV–visible scan spectra of solutions of $Mo_3O_4^{4+}$ (0.0012–0.06 M) in Hpts (0.03–2.00 M) [μ = 2.0 M (Li(pts)), 298.2 K (except for $[H^+] > 1.4$ M)].

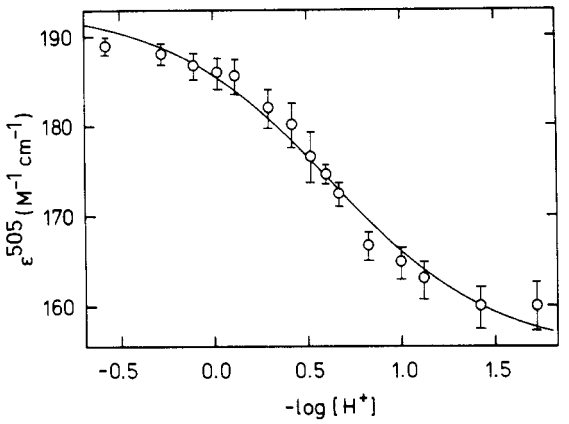

Figure 3. $[H^+]$ dependence of the extinction coefficient at the 505-nm peak for solutions of $[Mo_3O_4(OH_2)_9]^{4+}$ (conditions as in Figure 2). Bars denote estimated error limits.

Crystal Data and Data Collection for $[Mo_3O_4(OH_2)_9](CH_3C_6H_4SO_3)_4 \cdot 13H_2O$. $Mo_3S_4O_{38}C_{28}H_{72}$, mol wt 1432.9, monoclinic space group *Cc* (No. 9), a = 31.99 (1) Å, b = 9.886 (2) Å, c = 17.789 (5) Å, β = 99.67 (2)°, V = 5547 (3) Å^3, Z = 4, $F(000)$ = 2936, T = 240 K, ρ_{calc} = 1.72 g cm^{-3}, graphite-monochromatized Mo Kα radiation (λ = 0.71073 Å), μ(Mo Kα) = 11.54 cm^{-1}.

A sample of $[Mo_3O_4(H_2O)_9]^{4+}$ (0.013 M) in 1.00 M Hpts was observed to deposit dark-red crystals from the frozen solution after 6 months at ca. 253 K. A suitable dark red crystal was sealed in a Lindeman capillary tube and mounted on a Syntex R3m automatic four-circle diffractometer. All the handling operations were performed at the crystallization temperature: 250–255 K. Cell parameters were obtained from 37 accurately centered reflections with $15 \leq 2\theta \leq 30°$. 10136 intensities were recorded at 240 K up to 2θ = 55° with the θ–2θ scan technique, a width of 1.6°, and a variable scan speed ranging from 3.0 to 15.0° min^{-1}. The intensities of three standard reflections, monitored each 97 measurements, showed a decreasing of almost 4%, which was accounted for in the data reduction. The systematic absences *hkl* with $h + k$ odd and *h0l* with *l* odd indicated the possible space group *Cc* or *C*2/*c*. The compatibility of the number of molecules in the unit cell with the possible molecular symmetries and the statistical analysis of the data indicated the acentric group *Cc*. The space group symmetry was subsequently confirmed by refinement.

The intensities were corrected for Lorentz–polarization effects. Of the 7502 independent measurements in the Laue-symmetry *m*, 5183 reflections were considered as observed with $I \geq 3\sigma(I)$, where $\sigma(I)$ represents the estimated standard deviation from counting statistics. The internal consistency index was R_i = 0.025.

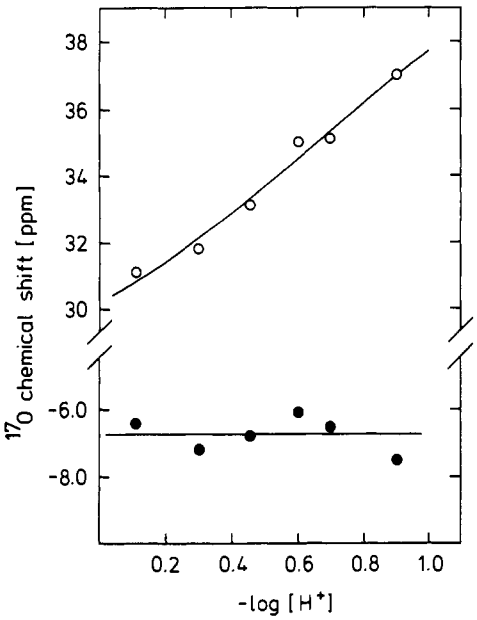

Figure 4. $[H^+]$ dependence of the ^{17}O chemical shift for the c-H_2O ligands of $[Mo_3O_4(OH_2)_9]^{4+}$ (0.01–0.04 M, $[H^+]$ = 0.125–0.900 M) trans to the μ_3-oxo groups (●) (δ_c = −6.7 ppm) and d-H_2O ligands trans to the μ_2-oxo groups (○) ($\delta_d(Mo_3O_4^{4+})$ = +24.1 ppm, $\delta_d(Mo_3O_4OH^{3+})$ = +39.4 ppm) (μ = 1.0 M (Li(tfms)), 298.2 K).

Table II. $[H^+]$ Dependence of the Exchange Rate of the Water Molecules of $[Mo_3O_4(OH_2)_9]^{4+}$ (0.01–0.04 M) Trans to the μ_3-Oxo Groups at 298.2 K [μ = 1.0 M (Li (pts))]

10^4k_{obsd}, s^{-1}	$[H^+]$, M	10^4k_{obsd}, s^{-1}	$[H^+]$, M
11.78	0.062	7.96	0.250
12.80	0.090	5.54	0.500
10.37	0.125	4.75	0.645
8.74	0.166		

Structure Determination for $[Mo_3O_4(OH_2)_9](CH_3C_6H_4SO_3)_4 \cdot 13H_2O$. The three independent Mo atoms were located on a sharpened three-dimensional Patterson map. Additional Fourier syntheses and a full-matrix least-squares refinement technique were used to complete the $[Mo_3O_4(OH_2)_9](CH_3C_6H_4SO_3)_4$ moiety. Additional Fourier maps showed many 3–5 e Å^{-3} residuals that could be interpreted, from stereochemical considerations, as the O atoms of 13 crystallization water molecules. This model is in agreement with the crystal growth conditions in which very little of the conjugate base (<10%) should be present. All the non-H atoms were refined anisotropically except for one μ_2-oxygen (O(4)), which showed a 0.7 e Å^{-3} residual at 0.9 Å. An attempt to interpret this density in terms of a disordered position of the O bridge was unsuccessful. Part of the water H atoms could be located on a weighted difference Fourier map. However, only the tosylate hydrogen atoms were introduced in the structure refinement, with calculated positions derived from geometrical considerations and fixed parameters (C–H = 1.08 Å and U = 0.040 Å^2). The final agreement converged to R = 0.059 and R_w = 0.054, with $w = \sigma^{-2}(F)$. On a final difference Fourier synthesis some electron density residuals (less than 1 e Å^{-3}) were observed at about 1 Å from the Mo atoms.

The fractional atomic coordinates with the equivalent isotropic displacement parameters of the non-H atoms are reported in Table I. Data reduction, structure solution, and drawings were performed with the SHELXTL-PLUS system (1987) from Nicolet XRD Co. on a μ-VAX II, while the structure refinement and the geometrical calculations were carried out with the SHELX76[18] and PARST[19] programs, respectively.

Results

Acid Dissociation Constant of $[Mo_3O_4(OH_2)_9]^{4+}$. Small rapid and reversible absorbance changes between 320 and 680 nm were observed for solutions of $[Mo_3O_4(OH_2)_9]^{4+}$ on rapidly lowering the $[H^+]$ between 2.0 and 0.02 M [μ = 2.0 M (Li(pts)), 298.2 K]. The resulting UV–visible spectra showed a notable decrease in the extinction coefficient at the 505-nm peak maximum with a small concurrent shift of the peak to higher energy (Figure 2). Isosbestic points, observed at 465 and 550 nm, confirmed that two simple trinuclear species were in equilibrium. Fitting the value of ϵ_{obs}^{505} as a function of $[H^+]$ to eq 1 (Figure 3) gave rise to the following adjustable parameters: $K_a^{298}(Mo_3O_4^{4+})$ = 0.24 ± 0.04 M, $\epsilon^{505}(Mo_3O_4^{4+})$ = 193 ± 1 M^{-1} cm^{-1}, and $\epsilon^{505}(Mo_3O_4OH^{3+})$ = 155 ± 2 M^{-1} cm^{-1}. Experimental errors resulting from the decreasing absorbance of Mo(IV) on dilution were estimated to reach ±10% and are shown in Figure 3. The decreased error in successive points around pH 0.5 is due to a change at that point from using a 0.1–1.0-cm path length quartz cell. The previously reported ϵ^{505} value of 189 M^{-1} cm^{-1}, at $[H^+]$ = 2.0 M,[13] is now consistent with the presence of ca. 5% of $[Mo_3O_4(OH_2)_8(OH)]^{3+}$. At $[H^+] \leq 0.02$ M, loss of the isosbestic points was observed concurrent with a general increase in absorbance (not now reversible) over the entire spectral range (320–680 nm) assigned to the formation of oligomeric oxygen-bridged products. When performed on ^{17}O enriched samples of $[Mo_3O_4(OH_2)_9]^{4+}$, such oligomer formation was further characterized by the appearance of a new ^{17}O resonance at +160 ppm assigned to a protonated bridging oxygen atom.

$[H^+]$ Dependence of the ^{17}O Chemical Shifts of the c- and d-H_2O Ligands. Klemperer has demonstrated that the ^{17}O chemical shifts of coordinated oxygen atoms are highly sensitive to their degree of protonation.[20,21] A shift to higher frequency of the ^{17}O resonance of a water ligand is indicative of deprotonation at that site. Figure 4 shows the respective ^{17}O chemical shifts for both the c- and d-H_2O ligands on $[Mo_3O_4(OH_2)_9]^{4+}$ as a function of $[H^+]$ in the range 0.125–0.900 M [μ = 1.0 M (Li(tfms)), 298.2 ± 0.5 K] as obtained by deconvolution of the two overlapping ^{17}O resonance lines. In this case Li(tfms) and not Li(pts) was used in order to supply a reference line not broadened by Mn^{2+} or shifted in the $[H^+]$ range studied. The same isotopically equilibrated $Mo_3O_4^{4+}$ solutions (0.01–0.04 M), following monitoring of the c-H_2O exchange, were used. An additional point at $[H^+]$ = 0.9 M and $[Mo_3O_4^{4+}]$ = 0.02 M is shown. Clearly deprotonation (high-frequency shift) only at the d-H_2O ligands is relevant within the range of $[H^+]$ studied. The variation in chemical shift for the d-H_2O ligands showed a satisfactory fit to eq 1 (Figure 4) with $\delta^{17}O$ replacing ϵ^{505}. Fixing K_a^{298} at 0.24 M gave, as adjustable parameters for the d-H_2O ligands, $\delta_d(Mo_3O_4^{4+})$ = +24.1 ± 0.7 ppm and $\delta_d(Mo_3O_4OH^{3+})$ = +39.4 ± 0.6 ppm, and for the c-H_2O ligands, δ_c = −6.7 ± 0.5 ppm. Owing to the high concentrations of $[Mo_3O_4(OH_2)_9]^{4+}$ used in the ^{17}O NMR measurements (≥0.02 M), meaningful data below $[H^+]$ = 0.125 M were not possible due to the rapid formation of oligomeric products.

Water Exchange at the μ_2 and μ_3 "Core" Oxygen Atoms. Contrary to an earlier report,[4] no exchange on either was detected over a 2-year period, and it was concluded that these oxygen atoms are kinetically inert, consistent with the known stability of this trinuclear metal cluster unit. A half life of >10 years seems relevant ($T \sim 295$ K). It should be added that, contrary to previously used ^{18}O isotopic labeling followed by mass spectrometry, ^{17}O NMR provides not only a uniquely selective and quantitative measure of the exchange rates at the different oxygen atoms in the case of oligomeric ions but allows one from the spectra to check the stability of them during the whole period of a kinetic run.

Water Exchange at the c-H_2O Ligands. The rate constants for the exchange at the c-H_2O ligand trans to the μ_3-oxo group were obtained by fitting the increase in intensity of its ^{17}O resonance line to a well-known function.[22] As reference, the resonance line of the d-H_2O ligands was used, which was already at isotopic equilibrium due to its much faster ($\sim 10^5$) exchange rate. The

(18) Sheldrick, G. M. "SHELX76, Program for crystal structure determination (version locally modified by F. Nicolò)", University of Cambridge, England, 1976; running on a VAX/8550 computer.
(19) Nardelli, M. *Comput. Chem.* **1983**, *7*, 95.
(20) Klemperer, W. G.; Shum, W. *J. Am. Chem. Soc.* **1977**, *99*, 3544.
(21) Day, V. W.; Klemperer, W. G.; Maltbie, D. J. *J. Am. Chem. Soc.* **1987**, *109*, 2991.
(22) Hugi-Cleary, D.; Helm, L.; Merbach, A. E. *Helv. Chim. Acta* **1985**, *68*, 545.

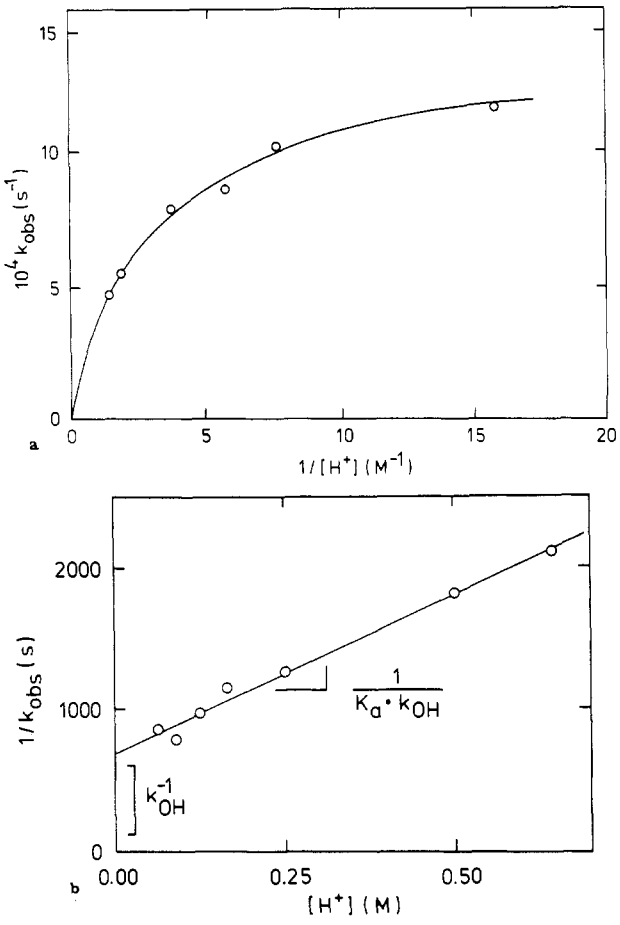

Figure 5. (a) Plot of k_{obs}^{298} for the c-H_2O exchange on $[Mo_3O_4(OH_2)_9]^{4+}$ (concentrations as in Table II) trans to the μ_3-oxo against $[H^+]^{-1}$ (hand drawn). (b) Linear plot of k_{obs}^{-1} against $[H^+]$ (least-squares computer fit).

exchange rate of the c-H_2O ligands was found to possess an inverse dependence on $[H^+]$ (Table II). Involvement of the conjugate base in the exchange mechanism was thus implied. However, consistent with the value of $K_a^{298}(Mo_3O_4^{4+})$ found above, the variation of k_{obs} with $[H^+]^{-1}$ was not linear with such plots, showing notable downward curvature (Figure 5a). The data were fitted to the dependence in eq 2[23] with $[H^+]$ comparable in magnitude

$$\frac{1}{k_{obs}} = \frac{1}{k_{OH}} + \frac{1}{K_a k_{OH}}[H^+] \qquad (2)$$

to K_a. The plot of k_{obs}^{-1} vs $[H^+]$ (Figure 5b) showed good linearity giving $k_{OH}^{298} = (1.5 \pm 0.9) \times 10^{-3}$ s^{-1} and $K_a^{298} = 0.31 \pm 0.04$ M.

Water Exchange at the d-H_2O Ligands. The much faster exchange of the d-H_2O ligands trans to μ_2-oxo results in line broadening of the corresponding ^{17}O NMR resonance. In order to separate the contributions due to the exchange kinetics from the ^{17}O quadrupolar relaxation, spectra of four samples at different acidities as a function of temperature were measured. The upper limit of temperature was kept to 339 K due to the rapid formation of oligomeric species at the higher values.[24]

The bound water region of the ^{17}O NMR spectra was fitted

(23) Equation 2 is in the form of $k_{obs} = (k_{ex}[H^+] + K_a k_{OH})/([H^+] + K_a)$, obtained by taking the reciprocal with k_{ex} set to 0. Attempts to fit the k_{ex} term, involving an exchange on the fully protonated ion, gave rise to a best fit of the data having $k_{ex} = 0$, and it was concluded that exchange occurred solely via the conjugate base $[Mo_3O_4(OH_2)_8(OH)]^{3+}$ involving deprotonation at a d-H_2O.

(24) Oligomerization of the Mo(IV) trimer to higher aggregates was indicated by a slight color change and a change of the 2:1 ratio for the intensities of the bound water signals. In oligomerized samples, this ratio became <2, indicating oligomerization at a deprotonated d-H_2O. The appearance of the +160 ppm resonance for $[H^+] \leq 0.02$ M, assigned to a μ_2-hydroxo group, was concurrent with the strong decrease of the d-H_2O resonance.

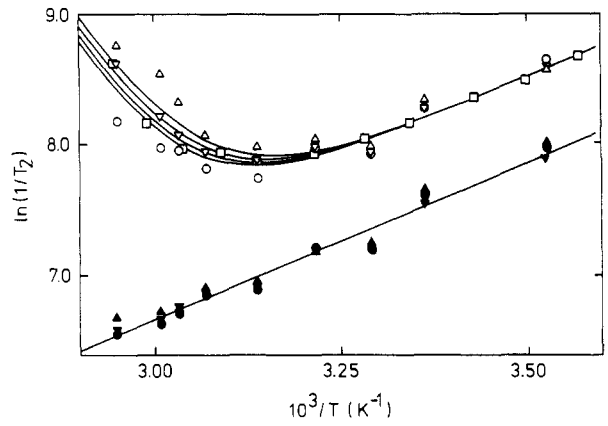

Figure 6. Temperature and $[H^+]$ dependence of the transverse relaxation rates ln $(1/T_2)$ for the ^{17}O resonances of the d-H_2O ligands of $[Mo_3O_4(OH_2)_9]^{4+}$ (0.02 M) trans to the μ_2-oxo groups (empty symbols) and c-H_2O ligands trans to the μ_3-oxo groups (filled symbols). The $[H^+]$ values are (○) 0.776, (□) 0.600, (▽) 0.500, and (△) 0.350 M; μ = 1.0 M (Li(pts)). The curves result from the simultaneous nonlinear least-squares fits as described in the text.

Table III. Results of the Water-Exchange Study on $[Mo_3O_4(OH_2)_9]^{4+}$ [μ = 1.0 M (Li (pts))]

	c-H_2O trans to μ_3-oxo	d-H_2O trans to μ_2-oxo
K_a^{298}, M		0.31 ± 0.04[a]
		0.24 ± 0.04[b]
k_{OH}^{298},[c] s^{-1}	(1.5 ± 0.9) × 10^{-3}	(1.6 ± 0.6) × 10^{+2}
$\Delta H^{\ddagger}$, kJ mol^{-1}		71.0 ± 8.5
$\Delta S^{\ddagger}$, J K^{-1} mol^{-1}		+35.2 ± 25.2
$1/T_{2Q}^{298}$, s^{-1}	(1.81 ± 0.04) × 10^{+3}	(3.52 ± 0.08) × 10^{+3}
E_Q, kJ mol^{-1}	19.7 ± 0.6	

[a] Obtained from the $[H^+]$ dependence of the exchange rate of the waters trans to the μ_3-oxo groups [μ = 1.0 M (Li (pts))]. [b] Obtained from UV–visible spectrophotometric measurements [μ = 2.0 M (Li (pts))]. [c] k_{OH} represents the rate constant for the exchange of a particular c- or d-H_2O molecule.[47]

to two Lorentzian lines by using a nonlinear least-squares program. The temperature and $[H^+]$ dependence of the transverse relaxation rate $1/T_2$ for both the slow-exchanging c-H_2O ligands and the fast-exchanging d-H_2O ligands are shown in Figure 6.

At $T > 315$ K the resonance line of d-H_2O ligands started to broaden with increasing temperature. The amount of broadening was also dependent strongly on the $[H^+]$ of the solution. In contrast to this it is evident from Figure 6 that the quadrupolar relaxation rate, $1/T_{2Q}$, for both resonances, being dominant for the c-H_2O ligands in the temperature range studied and, at low temperature ($T < 310$ K), also for the d-H_2O ligands, is $[H^+]$ independent. An Arrhenius temperature dependence was assumed for the quadrupolar relaxation rates (eq 3), where $1/T_{2Q}^{298}$ is the

$$\frac{1}{T_{2Q}} = \frac{1}{T_{2Q}^{298}}\left[\exp\left(\frac{E_Q}{R}\left(\frac{1}{T} - \frac{1}{298.2}\right)\right)\right] \qquad (3)$$

contribution at 298.15 K and E_Q is the corresponding activation energy. The parallel decrease of $1/T_{2Q}$ with temperature for both types of bound water reflects very similar activation energies, E_Q. The difference in the observed relaxation rates arises from the different quadrupolar coupling constants for the two sites.[25] For the kinetic exchange region, the temperature and $[H^+]$ dependence of the resulting water-exchange rate constant (d-H_2O) could then be satisfactorily described with the help of eq 4 and 5 with the

$$\frac{1}{T_{2obs}} = \frac{1}{T_{2Q}} + \frac{K_a k_{OH}}{K_a + [H^+]} \qquad (4)$$

$$k_{OH} = \frac{k_B T}{h}\left[\exp\left(\frac{\Delta S^{\ddagger}}{R} - \frac{\Delta H^{\ddagger}}{RT}\right)\right] \qquad (5)$$

(25) Abragam, A. *The Principles of Nuclear Magnetism*; Clarendon: Oxford, England, 1961.

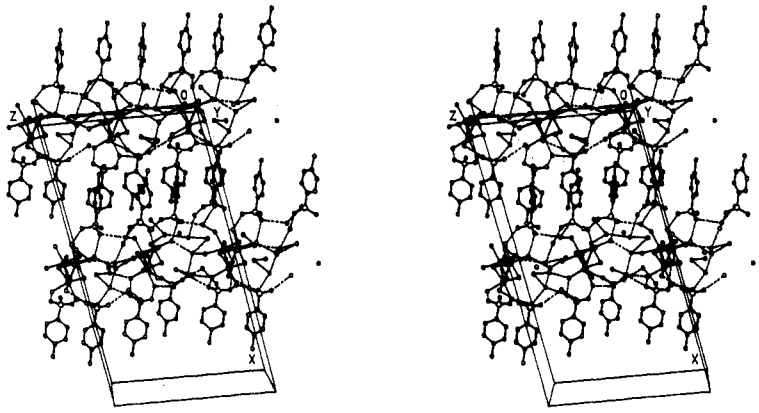

Figure 7. Stereoscopic view of the crystal packing with arbitrary atom radii. The hydrogen bonds are represented with dotted lines and the Mo atoms with dark circles. On the basis of chemical considerations, only O···O distances below 3.00 Å were reported as H bonds.

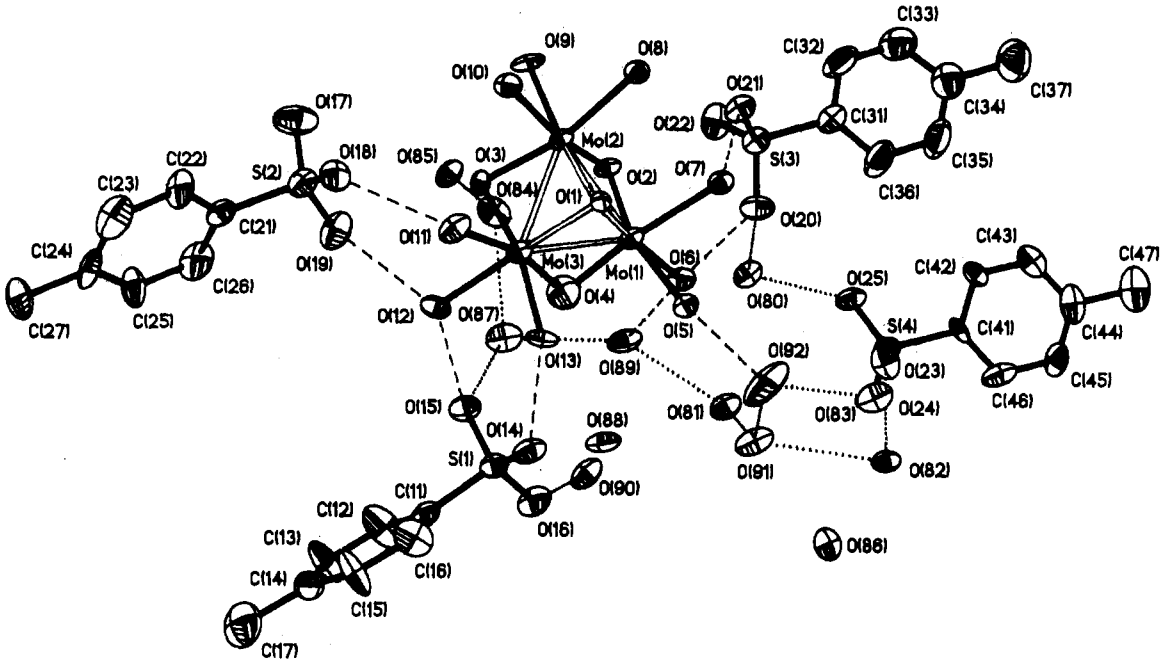

Figure 8. View of an asymmetric unit indicating the numbering scheme and showing the 13 crystallization water molecules. The hydrogen bonds are represented with dashed lines if they are linking coordinated H_2O molecules and with dotted lines if the contrary is true. Thermal ellipsoids include 50% probability, except O(1), which is represented by using an arbitrary scale.

same $[H^+]$ dependence as for the c-H_2O exchange. A nonlinear least-squares analysis of ln $(1/T_2)$ as a function of $[H^+]$ and temperature allowed a fit of the five parameters k_{OH}^{298} (or $\Delta S^{\ddagger}$), $\Delta H^{\ddagger}$, $1/T_{2Q}^{298}$ (trans to μ_3-oxo), $1/T_{2Q}^{298}$ (trans to μ_2-oxo), and E_Q (K_a was calculated at each temperature from $K_a^{298} = 0.24$ M and $\Delta H_a^0 = +30$ kJ mol^{-1} [26]). The curves belonging to the best fit are shown in Figure 6, and the corresponding adjusted parameters are given in Table III.

Structure Description and Discussion of $[Mo_3O_4(OH_2)_9](CH_3C_6H_4SO_3)_4 \cdot 13H_2O$. The solid compound is characterized by a large number of crystallization water molecules. This property is due the preparation of the crystals almost under the solidification conditions of the initial aqueous solution. At about 263 K, the solid phase starts to dissolve and a liquid appears with the same color.

The crystal packing can be described as an infinite series of layers parallel to the crystallographic (b,c) plane with alternating opposite charges (Figure 7). The positive stratum consists of the $[Mo_3O_4(OH_2)_9]^{4+}$ moieties interconnected and enveloped by the crystallization water molecules through a thick net of hydrogen bonds. The negative layer is formed by the tosylates oriented perpendicularly to the adjacent cationic planes. The negative $-SO_3^-$ poles are directed toward the cations and are involved in further H bonds with the crystallization water and the coordinated water molecules. Important bond distances and angles are reported in Table IV.

The asymmetric unit contains one molecule including a nucleus formed by the $[Mo_3O_4(OH_2)_9]^{4+}$ cluster and surrounded by four $CH_3C_6H_4SO_3^-$ anions. In addition, 13 noncoordinated water molecules are interposed between them and connect both ions with hydrogen bonds (Figure 8). This arrangement is quite similar to a hydrated cation surrounded by the counterions in an aqueous solution. The crystal packing is probably generated by a solidification process of the liquid phase in which many bulk water molecules are trapped in the resulting solid. An identical case was recently reported for $[W_3S_4(OH_2)_9](CH_3C_6H_4SO_3)_4$, which crystallizes at low temperature in a triclinic space group with seven H_2O-molecules.[28] This cluster seems to be more stable. A possible explanation lies in the different packing and amount of crystallization water depending on the more favorable conditions for the sulfur aqua ion.

The Mo_3O_4 cluster shows a very regular geometry (Figure 9).

(26) Nine known experimental values of ΔH_a^0 for aqua ions fall mainly within the range from +20 to +40 kJ mol^{-1}.[27] Least-squares analysis with ΔH_a^0 values between +10 and +60 kJ mol^{-1} gave $\Delta H^{\ddagger}$, $\Delta S^{\ddagger}$, and k_{OH}^{298} values for d-H_2O exchange that fall within the experimental errors given in Table III, assuming a ΔH_a^0 value of +30 kJ mol^{-1}.

(27) Burgess, J. *Metal Ions in Solution*; Ellis Horwood: Chichester, England, 1978; p 276.

(28) Shibahara, T.; Takeuchi, T.; Ohtsuji, A.; Kohda, K.; Kuroya, H. *Inorg. Chim. Acta* **1987**, *127*, L45.

Table IV. Selected Bond Lengths (Å) and Bond Angles (deg).

Mo(1)–Mo(2)	2.488 (2)	Mo(1)–Mo(3)	2.471 (2)	Mo(2)–Mo(3)	2.484 (2)
Mo(1)–O(1)	2.01 (1)	Mo(2)–O(1)	2.011 (9)	Mo(3)–O(1)	2.00 (1)
Mo(1)–O(2)	1.915 (9)	Mo(2)–O(2)	1.889 (9)	Mo(3)–O(3)	1.890 (9)
Mo(1)–O(4)	1.87 (1)	Mo(2)–O(3)	1.92 (1)	Mo(3)–O(4)	1.909 (9)
Mo(1)–O(5)	2.049 (9)	Mo(2)–O(8)	2.12 (1)	Mo(3)–O(11)	2.134 (9)
Mo(1)–O(6)	2.160 (9)	Mo(2)–O(9)	2.15 (1)	Mo(3)–O(12)	2.14 (1)
Mo(1)–O(7)	2.16 (1)	Mo(2)–O(10)	2.16 (1)	Mo(3)–O(13)	2.13 (1)
S(1)–O(14)	1.47 (1)	S(1)–O(15)	1.47 (1)	S(1)–O(16)	1.46 (1)
S(2)–O(17)	1.44 (1)	S(2)–O(18)	1.47 (1)	S(2)–O(19)	1.45 (1)
S(3)–O(20)	1.47 (1)	S(3)–O(21)	1.47 (1)	S(3)–O(22)	1.45 (1)
S(4)–O(23)	1.46 (1)	S(4)–O(24)	1.45 (1)	S(4)–O(25)	1.45 (1)
S(1)–C(11)	1.75 (2)	S(2)–C(21)	1.75 (2)	S(3)–C(31)	1.76 (2)
S(4)–C(41)	1.76 (1)	C(17)–C(14)	1.52 (3)	C(27)–C(24)	1.46 (2)
C(37)–C(34)	1.55 (3)	C(47)–C(44)	1.54 (3)	$(C–C)_{Ph}$	1.37 (3)
Mo(3)–Mo(1)–Mo(2)	60.11 (8)	Mo(3)–Mo(2)–Mo(1)	59.61 (7)	Mo(2)–Mo(3)–Mo(1)	60.28 (8)
Mo(2)–O(1)–Mo(1)	76.4 (3)	Mo(3)–O(1)–Mo(1)	75.9 (3)	Mo(3)–O(1)–Mo(2)	76.4 (3)
Mo(2)–O(2)–Mo(1)	81.7 (4)	Mo(3)–O(3)–Mo(2)	81.4 (4)	Mo(3)–O(4)–Mo(1)	81.6 (4)
O(1)–Mo(1)–Mo(2)	51.8 (3)	O(1)–Mo(2)–Mo(1)	51.8 (3)	O(1)–Mo(3)–Mo(1)	52.1 (3)
O(1)–Mo(1)–Mo(3)	52.0 (3)	O(1)–Mo(2)–Mo(3)	51.7 (3)	O(1)–Mo(3)–Mo(2)	51.9 (3)
O(5)–Mo(1)–Mo(3)	101.4 (3)	O(8)–Mo(2)–Mo(1)	98.1 (3)	O(11)–Mo(3)–Mo(2)	99.4 (3)
O(7)–Mo(1)–Mo(2)	92.5 (3)	O(10)–Mo(2)–Mo(3)	96.2 (3)	O(13)–Mo(3)–Mo(1)	95.6 (3)
O(2)–Mo(1)–O(1)	99.7 (4)	O(2)–Mo(2)–O(1)	100.6 (4)		100.6 (4)
O(4)–Mo(1)–O(1)	100.9 (4)	O(3)–Mo(2)–O(1)	99.5 (4)	O(4)–Mo(3)–O(1)	99.8 (4)
O(4)–Mo(1)–O(2)	96.1 (4)	O(3)–Mo(2)–O(2)	96.8 (5)	O(4)–Mo(3)–O(3)	97.6 (4)
O(5)–Mo(1)–O(1)	86.6 (4)	O(8)–Mo(2)–O(1)	88.8 (4)	O(11)–Mo(3)–O(1)	90.5 (4)
O(5)–Mo(1)–O(2)	163.1 (4)	O(8)–Mo(2)–O(2)	92.0 (4)	O(11)–Mo(3)–O(3)	90.5 (4)
O(5)–Mo(1)–O(4)	98.1 (4)	O(8)–Mo(2)–O(3)	166.6 (4)	O(11)–Mo(3)–O(4)	165.4 (4)
O(6)–Mo(1)–O(1)	169.4 (4)	O(9)–Mo(2)–O(1)	170.7 (4)	O(12)–Mo(3)–O(1)	171.0 (4)
O(6)–Mo(1)–O(2)	88.5 (4)	O(9)–Mo(2)–O(2)	85.6 (4)	O(12)–Mo(3)–O(3)	85.4 (4)
O(6)–Mo(1)–O(4)	84.6 (4)	O(9)–Mo(2)–O(3)	86.7 (4)	O(12)–Mo(3)–O(4)	85.9 (4)
O(6)–Mo(1)–O(5)	83.7 (4)	O(9)–Mo(2)–O(8)	83.9 (4)	O(12)–Mo(3)–O(11)	82.6 (4)
O(7)–Mo(1)–O(1)	91.3 (4)	O(10)–Mo(2)–O(1)	88.2 (4)	O(13)–Mo(3)–O(1)	89.4 (4)
O(7)–Mo(1)–O(2)	82.6 (4)	O(10)–Mo(2)–O(2)	168.6 (4)	O(13)–Mo(3)–O(3)	167.4 (5)
O(7)–Mo(1)–O(4)	167.7 (4)	O(10)–Mo(2)–O(3)	88.8 (4)	O(13)–Mo(3)–O(4)	88.1 (4)
O(7)–Mo(1)–O(5)	81.5 (4)	O(10)–Mo(2)–O(8)	80.9 (4)	O(13)–Mo(3)–O(11)	81.7 (4)
O(7)–Mo(1)–O(6)	83.2 (4)	O(10)–Mo(2)–O(9)	84.8 (4)	O(13)–Mo(3)–O(12)	83.8 (4)
$(C–C–C)_{Ph}$	120 (2)	O–S–O	112 (1)	O–S–C	107 (1)

The fragment has approximately a cubic arrangement with the capping O at the central vertex and the Mo atoms at the three adjacent ones. The μ_2-oxygens are at the other three vertices, diagonal to μ_3-O, on the three almost orthogonal faces defined by the Mo_3O fragment. Each Mo–(μ_3-O)–Mo plane contains the corresponding μ_2-O bridge and forms an average dihedral angle of 101 ± 0.5° with the other two faces (Table S6). The deformation from the regular cubic geometry is mainly due to the compression of the $Mo_3(\mu_3\text{-O})$ tetrahedron normal to the molybdenum plane. This is caused by the Mo–O bonds being significantly shorter than the Mo–Mo distances: 2.01 (1) Å vs 2.48 (1) Å, respectively. In the plane defined by the three Mo(IV) atoms, the metal–metal separation is characteristic for a single Mo–Mo bond interaction, as confirmed by the sum of the covalent radii (2.6 Å). The same value was observed by Cotton et al.[29] in the analogous (oxalato)trimolybdenum clusters. The authors pointed out that the Mo–Mo distances were shorter than the corresponding single-bond lengths reported for other complexes (2.53 Å) and explained this difference by the considerable influence of the metal neighborhood on the lower order bonds.

The three Mo(IV) atoms are practically equivalent in the range of the experimental errors. This is clearly indicated by the data in Table IV. Neglecting the two Mo–Mo bonds, each molybdenum coordination can be described by a distorted octahedron having two edges in common with the other two polyhedra. The Mo–O bond lengths are not equivalent and depend on the type of oxygen: 2.01 (1), 1.90 (1), and 2.13 (1) Å respectively for μ_3-O, μ_2-O, and water O atoms. The same observation was already reported by Rodgers et al., who found similar values in analogous clusters.[4] No discrimination could be done between the bonds with c- or d-H_2O.[30] From this consideration it is possible to conclude that the μ_3- and μ_2-oxygens are not significantly different as to cause a noticeable disparity in the opposite molybdenum–water bond lengths by corresponding trans effects. The Mo–H_2O bond lengths are significantly different however in an analogous trinuclear cluster having oxo and alkoxide bridges. The metal–water bonds, trans to the μ-OR ligands, are shorter than the Mo–H_2O opposite to the oxo bridge.[31] In these compounds the difference is clearly due to the trans influence oxo < OR.

Around the $[Mo_3O_4(OH_2)_9]^{4+}$ a solvation shell is formed by the crystallization water molecules and the tosylates, and H-bonds occur with the coordinated H_2O. Each coordinated water molecule is linked to two oxygens of either crystallization water or tosylate. The (coordination) oxygen–(solvation) oxygen distances fall in the range 2.52–2.74 Å (mean 2.65 ± 0.05 Å). The six d-H_2O ligands are connected to eight crystallization water molecules and four tosylate oxygens (Table S5). The three c-H_2O ligands are connected to three water molecules and three tosylate oxygens. The next O···O shortest distance is 3.11 Å. There is only one O···O distance below 3.00 Å for μ-O groups: μ_2-O(3) is linked to the crystallization water O(88) (2.84 Å) that is also connected to the c-water O(9) (2.73 Å), forming the sole observed H-interaction bridge between oxygen atoms of $[Mo_3O_4(OH_2)_9]^{4+}$.

Discussion

The first acid dissociation constant, K_a^{298}, of $[Mo_3O_4(OH_2)_9]^{4+}$ has been measured by UV–visible spectrophotometry, μ = 2.0 M (Li(pts)), and has a value of 0.24 M. Oxygen-17 NMR spectroscopy has shown that d-H_2O ligands, trans to μ_2-oxo (**2**), are involved in the deprotonation. Such high acidity is surprising given that the effective positive charge per Mo(IV) on this trinuclear ion is a mere 1.33. It is certainly not clear on electric grounds why this should be so. Cotton and colleagues have provided evidence from molecular orbital calculations in support of an

(29) Benory, E.; Bino, A.; Gibson, D.; Cotton, F. A.; Dori, Z. *Inorg. Chim. Acta* **1985**, *99*, 137.

(30) The significant shorter Mo(1)–O(5) bond could be related to the refinement problems of the μ_2-O(4) bridge linked to the same Mo atom.

(31) Chisholm, M. H.; Folting, K.; Huffman, J. C.; Kirkpatrick, C. C. *Inorg. Chem.* **1984**, *23*, 1021.

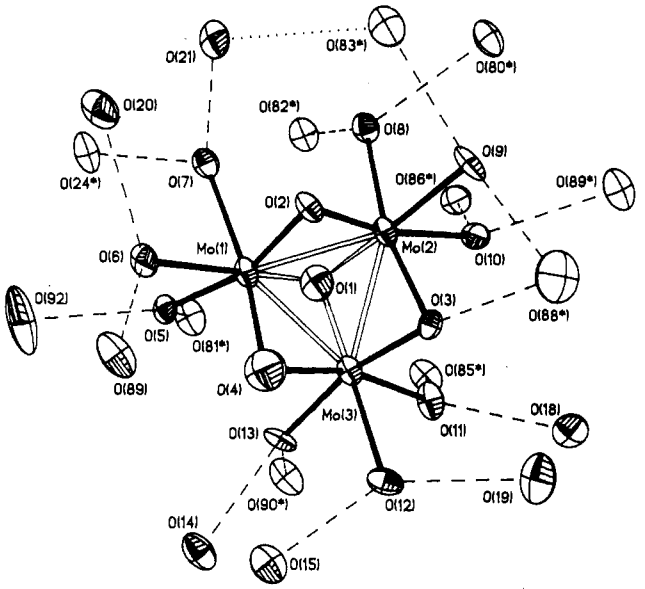

Figure 9. View of the $[Mo_3O_4(OH_2)_9]^{4+}$ moiety showing the numbering scheme and all the crystallization H_2O molecules and tosylate oxygens connected directly to the cation by hydrogen bonds (dashed lines). H bonds not linking coordinated water oxygens are represented with dotted lines. The asterisk denotes O atoms (white ellipsoids) of adjacent asymmetric units (Table S5). Thermal ellipsoids are represented with 50% probability, except O(1), which is represented by using an arbitrary scale.

involvement of the six d electrons in forming the triangular metal–metal-bonded framework.[32] The observation of only small

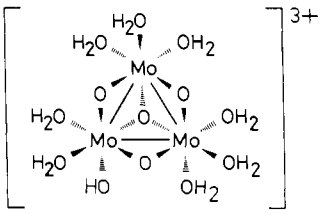

2

changes in the visible spectral chromophore of $[Mo_3O_4(OH_2)_9]^{4+}$, in the vicinity of the 505-nm peak maximum, on replacement of H_2O with OH^- (this work) and Cl^-,[33] supports further the molecular orbital picture derived by Cotton and colleagues as concluding that the relevant visible electronic transition is located within molecular orbitals involved with the metal–metal bonds and thus is little affected by the introduction of such σ- and π-donor ligands into the peripheral coordination sphere. The high acidity could then be explained by a resulting electron deficiency at each Mo(IV) center. Available empty π-acceptor orbitals on each Mo(IV) could then readily stabilize a deprotonated water ligand as in the case generally of electron-deficient high-oxidation-state metal ions. However, it is not at all clear why the first deprotonation occurs at a d-H_2O rather than at a c-H_2O. Interestingly, the X-ray structure does not reveal significant differences in Mo–OH_2 bond lengths, but it is recognized that a small change in bond length can have a dramatic effect on the strength of a H-bond and on the resulting solution properties.[34]

A reasonable alternative explanation for the high acidity could be through stabilization of the hydroxy ligand via intramolecular hydrogen bonding to produce an $H_3O_2^-$ bridging ligand. If intramolecular hydrogen bonding between two Mo(IV) centers is involved, it is clear that this would only be possible through interaction of d-H_2O ligands (**3**). The occurrence of such formally

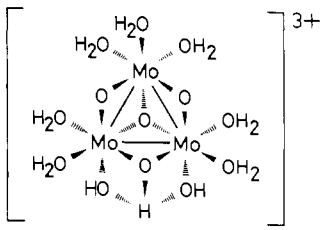

3

$H_3O_2^-$ bridging ligands is becoming increasingly relevant to the structural chemistry of many aqua–hydroxy derivatives of both mononuclear[34] and polynuclear[35,36] metal complexes. In addition, the presence of intramolecularly hydrogen-bonded hydroxy species has been found to correlate with anomalously high K_a values for the first deprotonation in several of these complexes.[35-37] Both linear and bent $H_3O_2^-$-bridged hydrogen bonds have been observed.[34] Formation of the bent $H_3O_2^-$ ligand envisaged here would necessitate the Mo–Mo–OH_2(d) angle to be $\leq 90°$ to enable the O–O distance between adjacent d-H_2O ligands, from different Mo atoms, to fall within the normal range for such hydrogen bonds (2.4–2.5 Å).[34] Formation of an intermolecular μ_2-($H_3O_2^-$) bridge between different trinuclear units[34] could be involved in the generation of the μ_2-hydroxo group assigned to the +160 ppm resonance observed in solutions of $Mo_3O_4^{4+}$ (0.04 M) at $[H^+] \leq 0.02$ M. The crystal structure of $[Mo_3O_4(OH_2)_9](CH_3C_6H_4SO_3)_4 \cdot 13H_2O$ does not however provide evidence that such a $H_3O_2^-$ bridge may form. All of the observed Mo–Mo–OH_2 angles are comparable and larger than 90° (mean O···O distances between adjacent d-H_2O ligands: 3.02 ± 0.11 Å). Furthermore there is no evidence of a crystallization water molecule bridging two adjacent d-H_2O ligands. It is recognized that the crystal structure may not necessarily represent a snapshot of the situation in solution and thus explanations of the high acidity as involving preferentially stronger H-bonds with the d-H_2O ligands in solution are possibilities that can still not be ruled out.

The present results for water exchange on $[Mo_3O_4(OH_2)_9]^{4+}$ have demonstrated the considerable kinetic inertness of *both* types of bridging oxygen atoms in the $Mo_3O_4^{4+}$ "core". The detection of somewhat higher lability at the μ_3-capping oxygen in the previous ^{18}O labeling studies of Murmann and colleagues[4,38] does not appear consistent with the present findings that imply a half-life of greater than 10 years for both.

Water exchange at the coordinated water ligands is however readily observed but with a rate that is highly dependent upon the location of the water ligand. Exchange at the d-H_2O ligands trans to the bridging μ_2-oxygens, occurs ca. 10^5 times faster than that at the c-H_2O ligands, trans to the μ_3 capping oxygen. Exchange at the c-H_2O ligands is slow enough to be monitored by conventional isotopic enrichment, using ^{17}O-NMR spectroscopy to follow the reaction. A mechanism solely involving the conjugate base $[Mo_3O_4(OH_2)_8(OH)]^{3+}$ is relevant, implying deprotonation of a d-H_2O ligand. Values for $K_a^{298}(Mo_3O_4^{4+})$ obtained from both kinetic (0.31 M) and spectrophotometric (0.24 M) measurements are in agreement within the experimental error. Water exchange at the d-H_2O ligands is also consistent with a kinetic path involving presumably the same conjugate base with deprotonation at a d-H_2O involving either one Mo(IV) center (**2**) or two Mo(IV) centers (**3**).

Such findings now have relevance to the anation studies performed on $[Mo_3O_4(OH_2)_9]^{4+}$ with regard to complexation with $HC_2O_4^-$ and NCS^- as incoming monodentate ligands.[12] Pathways solely involving the conjugate base form also appear relevant here with a kinetically determined $K_a^{298}(Mo_3O_4^{4+})$ value of 0.42 M,[12]

(32) Bursten, B. E.; Cotton, F. A.; Hall, M. B.; Najjar, R. C. *Inorg. Chem.* **1982**, *21*, 302.
(33) Electronic spectra of solutions of $[Mo_3O_4(OH_2)_9]^{4+}$ in 2.00 M HCl solution show only a small bathochromic shift in the peak maximum to 525 nm (no change in ϵ value) under conditions when appreciable quantities of $Mo_3O_4Cl^{3+}$ and $Mo_3O_4Cl_2^{2+}$ anated species are present.[4]
(34) (a) Ardon, M.; Bino, A. *Struct. Bonding (Berlin)* **1987**, *65*, 1. (b) Ardon, M.; Bino, A. *Inorg. Chem.* **1985**, *24*, 1343. (c) Ardon, M.; Bino, A.; Jackson, W. G. *Polyhedron* **1987**, *6*, 181. (d) Bino, A.; Gibson, D. *J. Am. Chem. Soc.* **1981**, *103*, 6741; **1982**, *104*, 4383.
(35) Christensson, F.; Springborg, J. *Inorg. Chem.* **1985**, *24*, 2129.
(36) Christensson, F.; Springborg, J. *Acta Chem. Scand., Ser. A* **1982** *A36*, 21.
(37) Galsbol, F; Larson, S.; Rasmussen, B.; Springborg, J. *Inorg. Chem.* **1986**, *25*, 290.
(38) Hinch, G. D.; Wycoff, D. E.; Murmann, R. K. *Polyhedron* **1986**, *5*, 487.

close to the values found in the present study. The question remains however as to at which site, c or d, does anation occur. For NCS^-, the available evidence favors anation at a d-H_2O ligand.[39] Monodentate anation of $HC_2O_4^-$ at a d-H_2O would also seem to correlate with the ultimate location of the chelating oxalate ligands at the d sites in the crystal structure of $[Mo_3O_4(C_2O_4)_3(OH_2)_3]^{2-}$.[3,4]

Rate constants for anation reactions on cationic aqua ions can generally be represented by $k_f = k_I K_{os}$,[40] where k_I represents the rate constant for the interchange step and K_{os} the outer-sphere ion-pair association constant. In order to decide whether the anation on the d site is dissociative or associative one can attempt to compare k_I and the water-exchange rate constant at that site. Such comparison requires the knowledge, or at least the magnitude of K_{os}. Its value, in the case of simple spherical ions, can be calculated by using the Fuoss model.[41] However, several groups[42] have highlighted the inadequacy of the model as applied to the case of nonspherical ion partners, which is highly relevant to the present study. For anation on $[Mo_3O_4(OH_2)_9]^{4+}$, the absence of detectable curvature in linear plots of k_{obs} against $[NCS^-]$ or $[HC_2O_4^-]$ in 10-fold excess up to 0.0035 M[10–12] suggests an upper limit of 10 M^{-1} for K_{os}. While calculations from the Fuoss model do not seem highly relevant, a lower limit of 0.5 M^{-1} for K_{os} can be estimated by assuming the incoming anion only interacting at one Mo(IV) center and thus only seeing formally a +0.33 charge at this deprotonated center (4.6 Å was taken as the distance of closest approach). This leads to a range between 0.4 and 8 s^{-1} for k_I by using an average value of 4 M^{-1} s^{-1} for k_f.[43] Such values, being somewhat smaller (~20 times) than the water-exchange rate constant, rules out an associative mechanism[44] at the d sites. The positive $\Delta S^{\ddagger}$ value (+35 J K^{-1} mol^{-1}) found here together with similar 1:1 anation rate constants found for NCS^- and $HC_2O_4^-$[12] are in support of a dissociative activation mode. A similar activation mode may also be relevant at the c sites.[45] The factor of 10^5 between the rate constants for water exchange at a d-H_2O as opposed to a c-H_2O, both cis conjugate base activated,[46] is probably a reflection of the much stronger trans effect of μ_2- vs μ_3-oxo groups, though it is surprising that this is not manifested through different Mo–OH_2 bond lengths. Such an indication of an I_d mechanism is initially surprising given the d^2 configuration of Mo(IV) but would not be inconsistent with the apparent coordination number of 8 per Mo if one includes the metal–metal-bonded framework.

The results presented have provided evidence for high acidity occurring for $[Mo_3O_4(OH_2)_9]^{4+}$ at the d-H_2O ligands (K_a^{298} = 0.24 M) trans to the μ_2-oxo groups. Such high acidity is surprising given that this Mo(IV) aqua ion is already in an extensively hydrolyzed state.

Water exchange at the c- and d-H_2O ligands proceeds only through the conjugate base ion, involving deprotonation of a d-H_2O, with rate constants for each that differ by 5 orders of magnitude; a behavior attributed to different trans effects of μ_2- and μ_3-oxo groups in the trinuclear ion. The μ_2- and μ_3-oxo groups of the "core" are extremely inert with a half-life >10 years for both suggested. The available evidence suggests that an I_d mechanism is relevant for water exchange at both sites and that initial complexation reactions occur exclusively through replacement of a d-H_2O.

Acknowledgment. We thank the Swiss National Science Foundation for supporting this research under Grant No 2.672-0.87 and Professor A. G. Sykes for helpful discussions and for supplying information prior to publication. D.T.R. wishes to thank the Nuffield Foundation and British Council for financial support. The Convention Intercantonale Romande pur l'Enseignement du Troisième Cycle en Chimie is also thanked for providing a visiting professorship in Lausanne to D.T.R.

Registry No. $[Mo_3O_4(OH_2)_9]^{4+}$, 74353-85-8; $[Mo_3O_4(OH_2)_9](CH_3C_6H_4SO_3)_4 \cdot 13H_2O$, 119390-73-7; H_2O, 7732-18-5.

Supplementary Material Available: Anisotropic displacement parameters (Table S1), calculated hydrogen positions (Table S2), complete bond lengths (Table S3) and bond angles (Table S4), O···O distances for the considered H-bond interactions (Table S5), and selected least-squares weighted planes and dihedral angles (Table S6) (8 pages); observed and calculated structure factors (Table S7) (36 pages). Ordering information is given on any current masthead page.

(39) In anation studies with excess NCS^-, two kinetically distinct isomeric forms of $[Mo_3O_4(NCS)]^{3+}$ have been identified involving possible NCS^- coordination independently at the c and d positions.[11] Isomer 1 is obtained following 1:1 anation and has the faster aquation rate, consistent with occupancy of the d position, with respect to isomer 2 obtained following aquation of $[Mo_3O_4(NCS)_2]^{2+}$. Occupancy of the c position is thought to arise during formation of $[Mo_3O_4(NCS)_2]^{2+}$. Anation at a d position was also favored by Murmann[4] following an observation that the rates of complexation by both Cl^- and $HC_2O_4^-$ were too fast to be consistent with the measured rate of water exchange at a c-H_2O.

(40) Eigen, M.; Wilkins, R. G. *Adv. Chem. Ser.* **1965**, *No. 49*, 55.
(41) Fuoss, R. M. *J. Am. Chem. Soc.* **1958**, *80*, 5059.
(42) See, e.g.: Sammes, G. G.; Steinfield, J. I. *J. Am. Chem. Soc.* **1962**, *84*, 4639; *J. Phys. Chem.* **1963**, *67*, 528.

(43) The values of $k_f \sim 4$ M^{-1} s^{-1} is an average value of the anation rate constants recently obtained from complexation of NCS^- (4.8 M^{-1} s^{-1}) and $HC_2O_4^-$ (3.3 M^{-1} s^{-1}) with $[Mo_3O_4(OH_2)_8(OH)]^{3+}$. The similarity of anation rate constants obtained here for both ligands was cited as evidence in favor of an I_d mechanism.[12]

(44) Associatively activated interchange steps have rate constants usually in excess of the water-exchange rate constants: Wilkins, R. G. *The Study of Kinetics and Mechanisms of Reactions of Transition Metal Complexes*; Allyn & Bacon: Boston, MA, 1974.

(45) A positive $\Delta S^{\ddagger}$ value of ~30 J K^{-1} mol^{-1} was found for water exchange at the c-H_2O on $[Mo_3O_4(OH_2)_9]^{4+}$.[4]

(46) (a) Tobe, M. L. *Adv. Inorg. Bioinorg. Mech.* **1983**, *2*, 48. (b) Henderson, R. A.; Tobe, M. L. *Inorg. Chem.* **1977**, *16*, 2576. (c) Buckingham, D. A.; Olsen, I. I.; Sargeson, A. M. *J. Am. Chem. Soc.* **1968**, *90*, 6539. (d) Nordmeyer, F. R. *Inorg. Chem.* **1969**, *8*, 2780.
(47) Swaddle, T. W. *Adv. Inorg. Bioinorg. Mech.* **1983**, *2*, 121.

Notes

Contribution from the Department of Chemistry, National Tsing Hua University, Hsinchu, Taiwan 30043, Republic of China

Effect of Ring Size on the Dissociation Kinetics of Copper(II)–Tetraamine Complexes

Lien-Huei Chen and Chung-Sun Chung*

Received August 17, 1988

A considerable amount of experimental material relating to the thermodynamics of transition-metal complexes with linear aliphatic tetraamines has been reported.[1–4] In particular for copper(II) complexes, it has been found that the stability of these complexes is dependent to a very large extent on the sizes of the three linked chelate rings.[2,5] It was of interest to see the effect of ring size on the dissociation kinetics of these copper(II) complexes.

(1) Weatherburn, D. C.; Billo, E. J.; Jones, J. P.; Margerum, D. W. *Inorg. Chem.* **1970**, *9*, 1557–1559.
(2) Barbucci, R.; Fabbrizzi, L.; Paoletti, P. *Coord. Chem. Rev.* **1972**, *8*, 31–37.
(3) Paoletti, P.; Fabbrizzi, L.; Barbucci, R. *Inorg. Chem.* **1973**, *12*, 1961–1962.
(4) Fabbrizzi, L.; Barbucci, R.; Paoletti, P. *J. Chem. Soc., Dalton Trans.* **1972**, 1529–1534.
(5) Chao, M.-S.; Chung, C.-S. *Inorg. Chem.* **1987**, *26*, 3600–3604.

